

# Intrahippocampal injection of a lentiviral vector expressing Nrf2 improves spatial learning in a mouse model of Alzheimer's disease

Katja Kanninen<sup>a</sup>, Riikka Heikkinen<sup>a</sup>, Tarja Malm<sup>a</sup>, Taisia Rolova<sup>a</sup>, Susanna Kuhmonen<sup>a</sup>, Hanna Leinonen<sup>b</sup>, Seppo Ylä-Herttua<sup>b</sup>, Heikki Tanila<sup>a,c</sup>, Anna-Liisa Levonen<sup>b</sup>, Milla Koistinaho<sup>a,d</sup>, and Jari Koistinaho<sup>a,e,1</sup>

Departments of <sup>a</sup>Neurobiology and <sup>b</sup>Biotechnology and Molecular Medicine, A. I. Virtanen Institute for Molecular Sciences, University of Kuopio, FI-70211 Kuopio, Finland; Departments of <sup>c</sup>Neurology and <sup>e</sup>Oncology, Kuopio University Hospital, FI-70211 Kuopio, Finland; and <sup>d</sup>Medeia Therapeutics Ltd., FI-70211 Kuopio, Finland

Communicated by Tomas Hökfelt, Karolinska Institutet, Stockholm, Sweden, July 31, 2009 (received for review February 24, 2009)

The amyloid hypothesis of Alzheimer's disease (AD) postulates that amyloid- $\beta$  (A $\beta$ ) deposition and neurotoxicity play a causative role in AD; oxidative injury is thought to be central in the pathogenesis. An endogenous defense system against oxidative stress is induced by binding of the transcription factor nuclear factor E2-related factor 2 (Nrf2) to the antioxidant response element (ARE) enhancer sequence. The Nrf2-ARE pathway is activated in response to reactive oxygen species to trigger the simultaneous expression of numerous protective enzymes and scavengers. To exploit the Nrf2-ARE pathway therapeutically, we delivered Nrf2 bilaterally into the hippocampus of 9-month-old transgenic AD mice (APP/PS1 mice) using a lentiviral vector encoding human Nrf2. The data indicate that significant reductions in spatial learning deficits of aged APP/PS1 mice in a Morris Water Maze can be achieved by modulating levels of Nrf2 in the brain. Memory improvement in APP/PS1 mice after Nrf2 transduction shifts the balance between soluble and insoluble A $\beta$  toward an insoluble A $\beta$  pool without concomitant change in total brain A $\beta$  burden. Nrf2 gene transfer is associated with a robust reduction in astrocytic but not microglial activation and induction of Nrf2 target gene heme oxygenase 1, indicating overall activation of the Nrf2-ARE pathway in hippocampal neurons 6 months after injection. Results warrant further exploration of the Nrf2-ARE pathway for treatment of AD and suggest that the Nrf2-ARE pathway may represent a potential therapeutic strategy to pursue in AD in humans, particularly in view of the multiple mechanisms by which Nrf2 can exert its protective effects.

amyloid-beta | astrocyte | heme oxygenase-1 | microglia | oxidative stress

Alzheimer's disease (AD) is a common age-associated dementia featuring progressive loss of neurons and synapses, gliosis, and the accumulation of intra- and extracellular protein deposits. The amyloid hypothesis of AD postulates that amyloid- $\beta$  (A $\beta$ ) deposition and neurotoxicity play a causative role in AD (1). Although the mechanisms through which A $\beta$  exerts its toxicity are numerous (2) and have not yet been fully elucidated, it seems that oxidative injury is central in the pathogenesis, even before the appearance of amyloid deposits (3, 4). The connection between AD and oxidative stress is apparent; A $\beta$  itself produces oxidative injury, prooxidants increase A $\beta$  production, and in AD brains the levels of expression and activities of several antioxidant enzymes are altered concomitantly with an increase in the appearance of markers of oxidative stress (5–7).

An endogenous defense system against oxidative stress is induced by binding of the transcription factor nuclear factor E2-related factor 2 (Nrf2) to the antioxidant response element (ARE) enhancer sequence (8–10). The Nrf2-ARE pathway is activated in response to reactive oxygen species and electrophilic agents to trigger the simultaneous expression of numerous protective enzymes and scavengers (11, 12). An essential step in the activation of the Nrf2-ARE pathway is the liberation of Nrf2

from the cytosolic repressor Keap1 (13), by means of which Nrf2 escapes proteasomal degradation and translocates to the nucleus to activate the expression of cytoprotective genes.

The potential role of the Nrf2-ARE pathway as a therapeutic target in AD is supported by the fact that Nrf2 levels are reduced in the hippocampus of AD patients (14). Moreover, in transgenic AD mice expressing mutated human amyloid precursor protein (APP) and presenilin 1 (PS1) genes (APP/PS1 mice), the Nrf2-ARE pathway is attenuated at the time of A $\beta$  deposition (15). Importantly, Nrf2 overexpression *in vitro* protects against neurotoxicity of A $\beta$  and is associated with increased expression of Nrf2 target genes and reduced oxidative stress (15, 16). In addition, it has been shown that curcumin and pyrrolidine dithiocarbamate, electrophilic compounds endowed with the capability to induce Nrf2, alleviate cognitive defects in transgenic animals modeling AD (17).

To exploit the Nrf2-ARE pathway therapeutically, we delivered Nrf2 directly to the hippocampus of APP/PS1 mice using a lentiviral vector encoding human Nrf2 (LV-Nrf2). Gene transfer of Nrf2 results in efficient and sustained Nrf2 expression in the hippocampus and improved spatial learning and memory of APP/PS1 mice. Our data demonstrate that intracerebral gene delivery of a molecule combating oxidative stress delays learning deficits in APP/PS1 mice, thus encouraging further exploration of the Nrf2-ARE pathway for the treatment of AD.

## Results

### Lentivirus-Mediated Expression of GFP and Nrf2 in the Hippocampus.

To investigate the efficiency and stability of our lentivirus-mediated transfer, we first analyzed the pattern of hippocampal GFP fluorescence in mice 6 months after GFP gene delivery. APP/PS1 and their WT littermates were administered the lentivirus vector encoding GFP (LV-GFP) or LV-Nrf2 bilaterally into the hippocampus at the age of 9 months and subsequently killed for analysis at the age of 15 months. In APP/PS1 mice administered LV-GFP, the GFP fluorescence was localized prominently at the injection site, at the dentate gyrus of the hippocampus (supporting information (SI) Fig. S1). Both cell bodies and mossy fibers projecting to the CA3 area were intensely labeled. In addition, GFP fluorescence was observed in the processes of CA3 pyramidal cells as well as granule and possibly some basket cells of the dentate gyrus. Staining of brain sections from GFP-injected mice with neuronal markers micro-

Author contributions: A.-L.L., M.K., and J.K. designed research; K.K., R.H., T.M., T.R., S.K., and H.L. performed research; S.Y.-H. contributed new reagents/analytic tools; K.K., R.H., T.M., H.T., A.-L.L., M.K., and J.K. analyzed data; and K.K., H.T., M.K., and J.K. wrote the paper.

The authors declare no conflict of interest.

<sup>1</sup>To whom correspondence should be addressed. E-mail: jari.koistinaho@uku.fi.

This article contains supporting information online at [www.pnas.org/cgi/content/full/0908397106/DCSupplemental](http://www.pnas.org/cgi/content/full/0908397106/DCSupplemental).

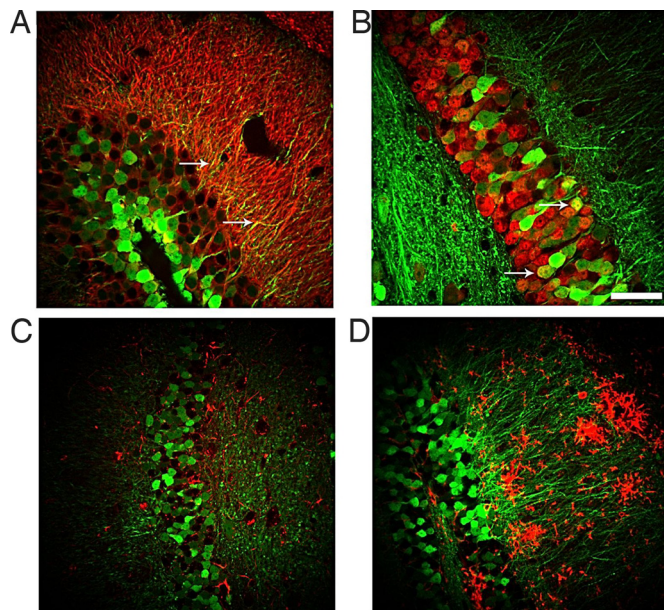


**Fig. 1.** Neurons are the primary cell type transduced by the LV-GFP vector. Confocal microscope images from brain sections of mice injected with LV-GFP stained with neuronal markers Map-2 (A) and NeuN (B) and glial markers GFAP (C) CD45 (D) 6 months after injection. Arrows point to colocalization of GFP fluorescence with cell-specific markers. (Scale bar, 50  $\mu$ m.)

tubule-associated protein-2 (Map-2) (Fig. 1A) and neuronal nuclei (NeuN) (Fig. 1B) revealed that neurons were the primary cell type transduced by the viral vector. There were no GFP-positive astrocytes or microglia, as assessed by immunostaining for glial fibrillary acidic protein (GFAP) (Fig. 1C) and CD45 (Fig. 1D), respectively. To determine whether lentiviral transduction of hippocampal neurons results in adverse cell loss or toxicity, we stained brain sections from some noninjected ani-

mals and all injection groups with neuronal marker NeuN and quantitatively assessed the immunoreactivity in the hippocampus (Fig. S2.) There was no histological evidence of neuronal injury in the hippocampus, indicating that there was negligible cytotoxicity caused by the lentiviral vector or the injection itself.

**Increased Nrf2 Levels in the Hippocampus of Nrf2-Injected APP/PS1 Mice.** We next investigated the mRNA expression level of human Nrf2 in the hippocampus of mice injected with the Nrf2-carrying lentiviral vector 6 months after injection. Human Nrf2 mRNA was readily detectable in APP/PS1 and WT mice injected with the vector. Interestingly, the expression level of human Nrf2 was 2.8 times higher in APP/PS1 animals than in the WT controls (Fig. S1). There was no detectable level of human Nrf2 in the GFP-injected mice. In addition, the mRNA levels of mouse Nrf2 and Keap1 were not altered due to injection of human Nrf2 into the hippocampus (Fig. S1 and Fig. S3). The activation of Nrf2 in nuclear and cytosolic fractions isolated from hippocampi was assessed by Nrf2 ELISA. The isolated nuclear fractions were positive for nuclear marker lamin B1 (Fig. S4). There was a slight increase in the amount of activated Nrf2 in the nuclear fractions of Nrf2-injected mice when compared with GFP-injected mice (mean OD 450 nm  $\pm$  SEM;  $0.375 \pm 0.013$  in Nrf2-treated vs.  $0.328 \pm 0.012$  in GFP-treated,  $P < 0.05$ ). A more prominent increase was evident in the cytosolic fractions ( $0.201 \pm 0.004$  in Nrf2-treated vs.  $0.151 \pm 0.003$  in GFP-treated,  $P < 0.001$ ).

**Neuronal HO-1 Expression Is Increased in Nrf2-Injected Mice.** Heme oxygenase-1 (HO-1), one of the target genes of Nrf2, is up-regulated in neurons after adenoviral transduction of Nrf2 in vitro (15). To investigate whether this potentially protective enzyme is also up-regulated in vivo after lentivirus-mediated gene transfer of Nrf2, we first analyzed the pattern of HO-1 immunoreactivity in the hippocampi of injected mice. As shown in Fig. 2A, a number of intensely stained HO-1 immunoreactive cells were localized primarily to the hilus of the dentate gyrus, the area of transgene injection. Importantly, these HO-1 immunoreactive cells were only seen in mice injected with the lentiviral

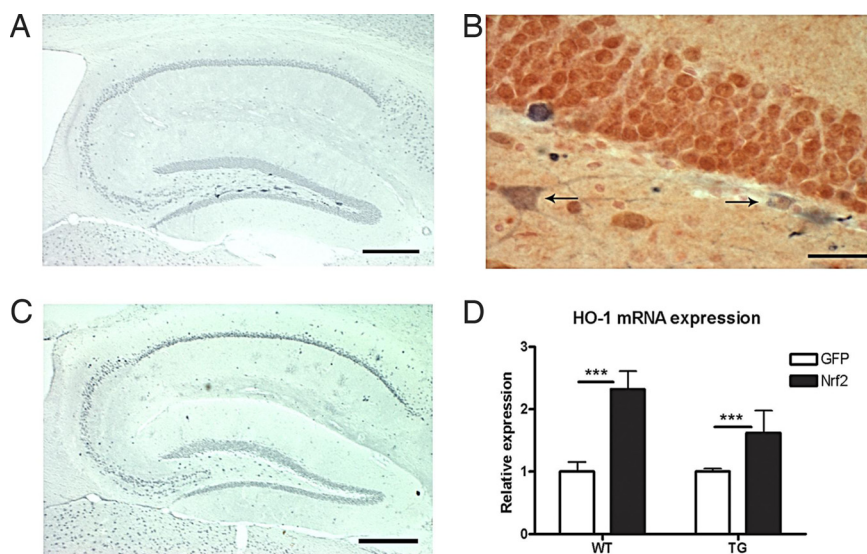


**Fig. 2.** LV-Nrf2 increases neuronal HO-1 expression 6 months after gene transfer. (A) Representative photomicrograph of HO-1 immunoreactivity in a brain section of a mouse injected with LV-Nrf2. Intense HO-1 staining is localized to the region of transgene injection. (Scale bar, 100  $\mu$ m.) (B) Representative photomicrograph of a brain section from a LV-Nrf2-injected mouse, double labeled by HO-1 (in blue) and NeuN (in red). Neurons are the primary HO-1-positive cell type. Arrows point to overlaid staining with the two antibodies. (Scale bar, 50  $\mu$ m.) (C) Representative photomicrograph of HO-1 immunoreactivity in a brain section of a mouse injected with LV-GFP. (Scale bar, 100  $\mu$ m.) (D) Increased mRNA expression of HO-1 in hippocampus of mice administered LV-Nrf2. HO-1 mRNA level is expressed as mean fold change normalized to ribosomal RNA  $\pm$  SEM (2-way ANOVA; \*\*\*,  $P < 0.001$ ;  $n = 6$  for WT-GFP and WT-Nrf2,  $n = 3$  for APP/PS1-GFP,  $n = 5$  for APP/PS1-Nrf2).





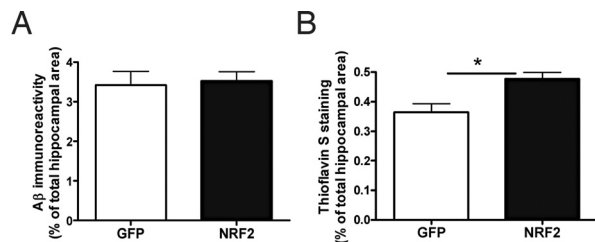


**Fig. 4.** LV-Nrf2 modifies A $\beta$  burden. (A) Quantification of pan-A $\beta$ -immunostained brain sections from APP/PS1 mice 6 months after injection of LV-GFP ( $n = 7$ ) or LV-Nrf2 ( $n = 8$ ). (B) Quantification of Thioflavin-S stained brain sections from APP/PS1 mice after injection of LV-GFP ( $n = 6$ ) or LV-Nrf2 ( $n = 6$ ) (Independent samples  $t$  test; \*,  $P < 0.05$ ). Data are presented as the percentage of area occupied by A $\beta$  immunoreactivity, and values represent means  $\pm$  SEM.

tein (GFAP) as an astrocytic marker (Fig. 5) and microgliosis using CD45 as a microglial marker (Fig. S6). As described previously, there was a clear increase in the amount of both astrogliosis and microgliosis in APP/PS1 mouse brain when compared with WT mouse brain (18). LV-Nrf2 treatment effectively attenuated the increase in GFAP immunoreactivity in the hippocampus of both WT and APP/PS1 mice (Fig. 5 A and B). Morphologically, it appeared that in Nrf2-injected mice, there was a reduction in thick, GFAP-positive processes in the area of transgene injection (Fig. S7). Overall, the GFAP immunoreactivity was reduced by 53% with Nrf2 injection in APP/PS1 mice. Although we were unable to demonstrate a significant change in GFAP mRNA level, in agreement with histological data, Nrf2 injection reduced the GFAP level by 52% in WT mice (Fig. S7). Nrf2 injection, however, did not alter the CD45

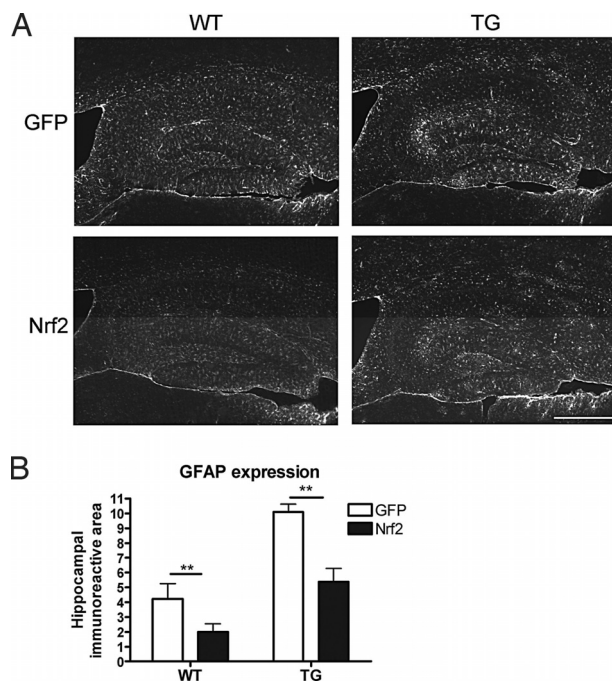


**Fig. 5.** APP/PS1 mice exhibit elevated astrogliosis that is attenuated by LV-Nrf2 treatment. (A) Representative photomicrographs of astrocytic GFAP immunostaining in hippocampus of mice injected with LV-GFP or LV-Nrf2. (Scale bar, 200  $\mu$ m.) (B) APP/PS1 mice exhibit elevated amounts of GFAP immunoreactivity. Astrocytosis is reduced 2-fold by LV-Nrf2 treatment. GFAP immunoreactivity is expressed as percentage of area occupied by the staining and is represented as means  $\pm$  SEM (2-way ANOVA; \*\*\*,  $P = 0.001$ ;  $n = 5$  for TG-Nrf2 and  $n = 6$  for WT-GFP, WT-Nrf2, and TG-GFP).

immunoreactivity in either APP/PS1 or WT hippocampus (Fig. S6). Correspondingly, the mRNA expression levels of tumor necrosis factor- $\alpha$  (TNF- $\alpha$ ) and interleukin 1 $\beta$  (IL-1 $\beta$ ) were elevated in APP/PS1 animals, yet were unaltered by LV-Nrf2 (TNF- $\alpha$  expression level normalized to ribosomal RNA: 708.8  $\pm$  158.4 in WT vs. 2123.3  $\pm$  611.2 in TG; IL-1 $\beta$  expression 515.2  $\pm$  107.9 in WT vs. 988.1  $\pm$  241.6 in TG).

## Discussion

The present study demonstrated that direct intrahippocampal gene delivery of Nrf2, a transcription factor central to the activation of an endogenous protective pathway combating oxidative stress, results in a reduction in spatial learning deficits in aged APP/PS1 mice. This study shows a beneficial behavioral outcome in APP/PS1 mice after gene transfer of a transcription factor. This behavioral improvement was seen when a lentiviral vector was used to deliver the Nrf2 gene into the hippocampus, an area of the brain directly affected by AD. Importantly, the gene delivery led to neuronal expression in the hippocampus lasting for at least 6 months, thus indicating the sustained nature of Nrf2 activation. The transgene expression was not only limited to neurons at the injection site but was diffusely distributed throughout the entire dentate gyrus and CA3 area with no histological evidence of neuronal injury. It is considered that the beneficial effect of Nrf2 induction in the central nervous system is based on the actions of astrocytes (19, 20), however, our study demonstrates that reductions in spatial learning deficits of aged APP/PS1 mice can be achieved by modulating levels of Nrf2 specifically in neurons.

Nrf2 has a relatively rapid turnover (half-life <20 min), and its activity is regulated by the repressor protein Keap1, which targets Nrf2 for proteosomal degradation (21, 22). Analysis of both the expression level of Nrf2 mRNA and the activation of Nrf2 in nuclear and cytosolic fractions isolated from hippocampus revealed a potent up-regulation after LV-Nrf2 treatment. The fact that abundant Nrf2 is present both in nucleus and cytoplasm suggests that the transduced cells possess an excess of Nrf2, which most likely saturates Keap1 and leads to the accumulation of Nrf2 in the nucleus with resulting induction of cytoprotective gene expression. This suggestion is supported by the finding that Keap1 expression levels were unaltered by transduction with lenti-Nrf2. In fact, the expression of HO-1, a cytoprotective enzyme involved in degradation of prooxidant heme to antioxidant bile pigments (23), was found to be induced in the area of transgene injection. We saw an increase in HO-1 immunoreactivity in a subpopulation of cells localized near the injection site that colocalized with the neuronal marker NeuN. Importantly, HO-1-positive neurons were found in animals treated with LV-Nrf2 regardless of genotype, but none were found in the animals treated with the control vector. This finding is in line with previous studies showing that HO-1 levels in the brain are controlled and up-regulated by Nrf2 activation (15). It is unlikely that the Nrf2-induced reduction in learning and memory deficits in APP/PS1 mice was mediated by increased HO-1 expression (24); rather, the induced HO-1 expression should be taken as an indication of complete activation of the Nrf2-ARE pathway in hippocampal neurons after Nrf2 gene transfer to WT and APP/PS1 mice.

Although we discovered an increased expression of GFP and hNrf2 mRNAs in APP/PS1 mice compared with WT mice 6 months after gene transfer, the levels of HO-1 mRNA and protein expression were similar in both mice. We did not detect evident differences in the extent or distribution of GFP expression between WT and APP/PS1 mice, even though we cannot exclude the possibility that the copy number of the transduced genes per cell may for some reason be higher in APP/PS1 mice in comparison with WT mice. Whereas the reason for differential hNrf2 mRNA expression between APP/PS1 and WT mice



remains unknown, the results show that the hippocampi of WT and APP/PS1 mice had comparable expression of HO-1 gene and protein, indicating that overall activation of the Nrf2-ARE pathway may be similarly extensive in both WT and APP/PS1 mice.

Memory improvement in APP/PS1 mice after Nrf2 transduction occurred with a slight, concomitant increase in brain A $\beta$  plaque burden, and this increase was associated with a 30% reduction in soluble forms of A $\beta$ 1–40 and A $\beta$ 1–42. Although the changes observed in soluble A $\beta$  were statistically insignificant, the A $\beta$  ELISA together with Thioflavin-S staining results suggest that gene delivery of Nrf2 into the hippocampus may result in a reduced shift of A $\beta$  toward soluble forms. Whether such a mild change is sufficient to explain the improved cognitive functions of APP/PS1 mice remains unclear. The effect of Nrf2 is most likely not based on A $\beta$  clearance by glial cells, because the total amount of brain A $\beta$  was not reduced. This idea is further corroborated with findings that astrogliosis was reduced in Nrf2-injected mice, and microgliosis was unaltered in GFP- and Nrf2-injected mice, suggesting no clear changes in microglial activation. Because a slight hint for improved performance of Nrf2-treated WT mice was seen in the MWM, overexpression of Nrf2 in hippocampal neurons could also be beneficial in aged WT mice.

The fact that we did not observe a reduction in microgliosis concomitant with improved spatial learning and memory indicates that microglia-mediated inflammation or A $\beta$  clearance may not be involved in the reduction of spatial learning deficits induced by Nrf2 gene transfer to 9-month-old APP/PS1 mice. This finding is of interest as microglial functions are closely related to oxidative stress (25) and thereby potentially to the Nrf2-ARE pathway (26). Recent reports on the use nonsteroidal antiinflammatory drugs (NSAIDs) (27–29), especially the evidence that the NSAIDs capable of directly modulating  $\gamma$ -secretase activity seem to prevent or slow the onset of AD (27, 28) supports the conclusion that even though possible A $\beta$  clearance by activated microglia may be beneficial, microglial activation in terms of released proinflammatory molecules may not have a crucial role in AD pathology and memory deficits. In contrast, astrocyte activation was robustly reduced by Nrf2 treatment; GFAP immunoreactivity was reduced by  $\approx$ 50% in both WT and APP/PS1 mice. LV-Nrf2 treatment also appeared to alter astrocyte morphology, as thick GFAP-immunoreactive processes were less frequently seen in Nrf2-injected animals. The mechanism by which increased Nrf2 expression in neurons results in reduced GFAP immunoreactivity, a marker of astrocytosis, is unclear. Nrf2 regulates a number of cytokines and growth factors that affect astroglial functions, including those involved in astroglial proliferation. For example, transforming growth factor  $\beta$ 1 (TGF- $\beta$ 1) is a Nrf2-regulated cytokine that reduces proliferation of astrocytes (30–33). It is thus possible that increased neuronal Nrf2 expression may result in synthesis and release of proteins that eventually reduce astrogliosis during the 6-month follow-up time. In addition, our results show that astrogliosis may in addition or instead be a consequence of altered neuronal function.

In summary, our data indicate that significant reductions in spatial learning deficits of aged APP/PS1 mice can be achieved by modulating levels of Nrf2 in the brain. This may represent a potential therapeutic strategy to pursue in AD in humans, particularly in view of the multiple mechanisms by which Nrf2 can exert its protective effects. In the future, the use of inducible promoters may provide control of gene expression required for time- and location-specific therapeutic treatment strategies. In addition, as more is understood about the biochemical pathways that regulate Nrf2, the more likely it is that specific inducers of the Nrf2-pathway are targeted for therapeutic benefit in neurodegenerative diseases.

## Materials and Methods

**Animals.** The transgenic APP/PS1 mice modeling AD were created by coinjection of chimeric mouse/human APP695 harboring the Swedish mutation and human PS1-dE9 vectors (34). The mice were back-crossed to C57BL/6J mice for 11 generations to create APdE9 mice in C57BL/6J background. WT siblings were used as controls. All mice used in this study were male. All animal work was approved by the State Provincial Office of Eastern Finland and performed according to the guidelines of the National Institutes of Health for animal care.

**Viral Vectors.** For lentiviral gene transfer, enhanced GFP- (35) and Nrf2-expressing lentiviruses under the control of human phosphoglycerate kinase promoter were used. LV-Nrf2 was cloned by digesting Nrf2 from pCI-Nrf2 (36) with NheI and SalI and then half-blunt ligating it into the BamHI-SalI site of the LV-GFP, displacing GFP. The lentiviruses were produced and titrated as described (37). The lentiviral vectors coding for GFP were used as a control.

**Intracerebral Administration of Viral Vectors.** At the age of 9 months, when A $\beta$  deposits are readily detected in the brain, APP/PS1 mice and their WT littermates were anesthetized with isoflurane and placed in a stereotaxic frame (model 940; David Kopf). Before injections, lentiviral vectors were diluted with sterile PBS (pH 7.4) to achieve a titer of  $1.71 \times 10^9$ . Viral preparations in 2- $\mu$ L volume were injected bilaterally into the dentate gyrus region of the hippocampus by using the following coordinates:  $\pm$ 3.2 mm medial/lateral,  $-2.7$  mm anterior/posterior,  $-2.7$  mm dorsal/ventral from the bregma. The preparation was injected with a speed of 0.5  $\mu$ L/min over a period of 4 min by using a Hamilton 5- $\mu$ L syringe and a 27 G needle. Before waking, mice received 0.05 mg/kg of buprenorphine s.c. (Temgesic 0.3 mg/mL) and were allowed to recover in a heated chamber.

**Behavioral Testing.** The effect of gene transfer on spatial learning and memory was assessed by MWM at the age of 15 months. The 5-day testing protocol used has been described in detail previously (18). Briefly, mice had 1 day of pretraining to climb the escape platform in a closed alley after which they underwent a 5-day testing phase with a submerged platform (10  $\times$  10 cm) in a circular black pool (diameter 120 cm) filled with water. During the procedure, the platform location was kept constant, and the starting points were varied between four constant locations on the pool rim. The acquisition phase (days 1–4) consisted of five trials in which the mice had a maximum of 60 s to find the platform, followed by a 10-s rest time on the platform after each trial. On the fifth day, the trial duration was reduced to 40 s, and for the last trial, the platform was removed to determine the search bias. Throughout the experiment, the mice had at least 1-min resting time between trials in a warmed cage. The time to find the platform and the length of the swim path were monitored and recorded semiautomatically by a tracking system connected to an image analyzer (HVS Image).

**Histochemistry.** Six months after vector injection, mice were deeply anesthetized with avertin and transcardially perfused with heparinized saline. After dissection, the left hemisphere was immersion-fixed in paraformaldehyde for 21 h. After cryoprotection, the hemisphere was frozen in liquid nitrogen and cut in 20- $\mu$ m cryosections with an interval of 400  $\mu$ m. The right hemisphere was dissected into hippocampal and cortical samples and either snap-frozen in liquid nitrogen or used freshly for measurement of Nrf2 A $\beta$  levels by ELISA. Activation and proliferation of astrocytes and microglia were assessed after immunostaining with GFAP (1:500; DakoCytomation) and CD45 (1:100; Serotec), respectively. Immunostaining for NeuN (1:200; Chemicon International) and Map-2 (1:100; Chemicon International) were carried out to assess the possible neurotoxicity of the gene transfer. Brain sections from noninjected mice were used as controls. Human A $\beta$  was detected with pan-A $\beta$  antibody (1:300; BioSource). The Alexa Fluor 568-conjugated secondary antibody for the above-mentioned stainings was obtained from Invitrogen (1:200). The HO-1 antibody was obtained from Stressgen (1:1,000). Primary antibody binding was visualized either by using an Alexa Fluor 568-conjugated secondary antibody (1:200; Invitrogen) or by biotinylated secondary antibodies (1:200; Vector Laboratories), avidin-biotin complex, and by using nickel-enhanced diaminobenzidine (Ni-DAB; Sigma-Aldrich) or NovaRED (Vector Laboratories) as substrate. Brain sections from APP/PS1 animals were stained with fresh, filtered, aqueous 1% Thioflavin-S. The hippocampal area from three to six sections in 400- $\mu$ m intervals throughout the hemisphere was evaluated per animal. For quantification of the immunoreactive areas, the sections were imaged with an Olympus AX70 microscope equipped with a digital camera (Color View 12 or F-view; SoftImaging Systems) or a confocal microscope (BioRad Radiance Laser Scanning Systems 2100; Bio-Rad Microscience) running

LaserSharp 2000 software (Bio-Rad Microscience). The immunoreactive area was quantified by using ImagePro Plus software (Media Cybernetics). Data are expressed as the area of hippocampi occupied by immunoreactivity and represented as the mean percentage  $\pm$  SEM.

**Quantitative Real-Time PCR.** One microgram of total RNA was used for cDNA synthesis using random hexamer primers (Promega) and M-MuLV reverse transcriptase (New England Biolabs). The relative expression levels of mRNA encoding human Nrf2, mouse Nrf2, Keap1, HO-1, GFAP, TNF- $\alpha$ , and IL-1 $\beta$  were measured according to manufacturer's protocol by quantitative RT-PCR (ABI PRISM 7700 Sequence detector; Applied Biosystems) by using specific assays-on-demand (Applied Biosystems) target mixes. The expression levels were normalized to ribosomal RNA and presented as fold change in the expression  $\pm$  SEM.

**Nuclear Fractionation and Western Blot Analysis.** Nuclear fractions were isolated from fresh hippocampal tissue according to Ogita et al. (38). To ensure the purity of the isolated nuclear fractions, proteins were separated on 10% SDS/PAGE gels with Mini Protean III apparatus (Bio-Rad) and transferred to PVDF membrane (GE Healthcare) using Mini Transblot Electrophoretic Transfer Cell Equipment (Bio-Rad). The membrane was incubated overnight with rabbit anti-lamin B1 (Abcam), HRP-conjugated Ig anti-rabbit at 1:3,000 (GE Healthcare) for 2 h, and developed by using enhanced chemiluminescence

(ECL+ kit; GE Healthcare). The membrane was visualized by using Storm 860 Fluorimager (GE Healthcare).

**A $\beta$  and Nrf2 ELISA.** The levels of A $\beta$ <sub>1-40</sub> and A $\beta$ <sub>1-42</sub> were analyzed by ELISA from freshly frozen hippocampal samples. For detection of A $\beta$  levels, the homogenized hippocampi were centrifuged for 1 h at 48,000  $\times$  g at 4  $^{\circ}$ C, and the supernatant was taken for the analysis of soluble A $\beta$  species, whereas the remaining pellet was suspended in 5 M guanidine-HCl/50 mM Tris-HCl, pH 8.0. The levels of A $\beta$ <sub>1-40</sub> and A $\beta$ <sub>1-42</sub> were quantified by using Signal Select Beta Amyloid ELISA kits (Biosource International) according to manufacturer's protocol. The level of total A $\beta$ <sub>1-40</sub> and A $\beta$ <sub>1-42</sub> was standardized to tissue weight and expressed as nanograms of A $\beta$  per gram  $\pm$  SEM. The level of Nrf2 was quantified from freshly isolated nuclear and cytosolic fractions (38) by using a TransAM Nrf2 ELISA kit according to manufacturer's instructions (Active Motif). The protein concentration of isolated fractions was measured by the Bio-Rad protein assay before analysis by ELISA. The Nrf2 level is expressed as OD450 nm  $\pm$  SEM.

**Statistical Analysis.** The data were analyzed by using *t* test or ANOVA in SPSS software, and statistical significance was assumed if *P* < 0.05.

**ACKNOWLEDGMENTS.** We thank Mrs. Mirka Tikkanen, Ms. Laila Kaskela, and Mrs. Raisa Giniatullina for their expert technical assistance. The study was supported by Finland's Academy, Sigrid Juselius Foundation, and the Institute for the Study of Aging.

- Hardy JA, Higgins GA (1992) Alzheimer's disease: The amyloid cascade hypothesis. *Science* 256:184–185.
- Crouch PJ, et al. (2008) Mechanisms of A beta mediated neurodegeneration in Alzheimer's disease. *Int J Biochem Cell Biol* 40:181–198.
- Selkoe DJ (2001) Alzheimer's disease: Genes, proteins, and therapy. *Physiol Rev* 81:741–66.
- Resende R, et al. (2008) Brain oxidative stress in a triple-transgenic mouse model of Alzheimer disease. *Free Radical Biol Med* 44:2051–7.
- Butterfield DA, et al. (2007) Roles of amyloid beta-peptide-associated oxidative stress and brain protein modifications in the pathogenesis of Alzheimer's disease and mild cognitive impairment. *Free Radical Biol Med* 43:658–677.
- Choi J, et al. (2005) Oxidative modifications and aggregation of Cu,Zn-superoxide dismutase associated with Alzheimer and Parkinson diseases. *J Biol Chem* 280:11648–11655.
- Chauhan V, Chauhan A (2006) Oxidative stress in Alzheimer's disease. *Pathophysiology* 13:195–208.
- Itoh K, et al. (1997) An Nrf2/small Maf heterodimer mediates the induction of phase II detoxifying enzyme genes through antioxidant response elements. *Biochem Biophys Res Commun* 236:313–322.
- Moi P, et al. (1994) Isolation of NF-E2-related factor 2 (Nrf2), a NF-E2-like basic leucine zipper transcriptional activator that binds to the tandem NF-E2/AP1 repeat of the beta-globin locus control region. *Proc Natl Acad Sci USA* 91:9926–9930.
- Wang J, et al. (2007) Role of Nrf2 in protection against intracerebral hemorrhage injury in mice. *Free Radical Biol Med* 43:408–414.
- Liu Y, et al. (2007) A genomic screen for activators of the antioxidant response element. *Proc Natl Acad Sci USA* 104:5205–10.
- Nguyen T, Sherratt PJ, Pickett CB (2003) Regulatory mechanisms controlling gene expression mediated by the antioxidant response element. *Annu Rev Pharmacol Toxicol* 43:233–260.
- Itoh K, et al. (1999) Keap1 represses nuclear activation of antioxidant responsive elements by Nrf2 through binding to the amino-terminal Neh2 domain. *Genes Dev* 13:76–86.
- Ramsey CP, et al. (2007) Expression of Nrf2 in neurodegenerative diseases. *J Neuro-pathol Exp Neurol* 66:75–85.
- Kanninen K, et al. (2008) Nuclear factor erythroid 2-related factor 2 protects against beta amyloid. *Mol Cell Neurosci* 39:302–313.
- Wruck CJ, et al. (2008) Kavalactones protect neural cells against amyloid beta peptide-induced neurotoxicity via extracellular signal-regulated kinase 1/2-dependent nuclear factor erythroid 2-related factor 2 activation. *Mol Pharmacol* 73:1785–1795.
- Frautschy SA, et al. (2001) Phenolic anti-inflammatory antioxidant reversal of Abeta-induced cognitive deficits and neuropathology. *Neurobiol Aging* 22:993–1005.
- Malm TM, et al. (2007) Pyrrolidine dithiocarbamate activates Akt and improves spatial learning in APP/PS1 mice without affecting beta-amyloid burden. *J Neurosci* 27:3712–3721.
- Johnson JA, et al. (2008) The Nrf2-ARE pathway: An indicator and modulator of oxidative stress in neurodegeneration. *Ann NY Acad Sci* 1147:61–69.
- Chen PC, et al. (2009) Nrf2-mediated neuroprotection in the MPTP mouse model of Parkinson's disease: Critical role for the astrocyte. *Proc Natl Acad Sci USA* 106:2933–2938.
- Stewart D, et al. (2003) Degradation of transcription factor Nrf2 via the ubiquitin-proteasome pathway and stabilization by cadmium. *J Biol Chem* 278:2396–2402.
- McMahon M, et al. (2003) Keap1-dependent proteasomal degradation of transcription factor Nrf2 contributes to the negative regulation of antioxidant response element-driven gene expression. *J Biol Chem* 278:21592–21600.
- Ponka P. (1999) Cell biology of heme. *Am J Med Sci* 318:241–256.
- Morgan D, et al. (1998) Impaired spatial navigation learning in transgenic mice over-expressing heme oxygenase-1. *Brain Res* 808:110–112.
- Sastre M, Klockgether T, Heneka MT (2006) Contribution of inflammatory processes to Alzheimer's disease: Molecular mechanisms. *Int J Dev Neurosci* 24:167–176.
- Innamorato NG, et al. (2008) The transcription factor Nrf2 is a therapeutic target against brain inflammation. *J Immunol* 181:680–689.
- Eriksen JL, et al. (2003) NSAIDs and enantiomers of flurbiprofen target gamma-secretase and lower Abeta 42 in vivo. *J Clin Invest* 112:440–449.
- Weggen S, et al. (2003) Evidence that nonsteroidal anti-inflammatory drugs decrease amyloid beta 42 production by direct modulation of gamma-secretase activity. *J Biol Chem* 278:31831–31837.
- Szekely CA, et al. (2008) No advantage of A beta 42-lowering NSAIDs for prevention of Alzheimer dementia in six pooled cohort studies. *Neurology* 70:2291–2298.
- Lindholm D, et al. (1992) Transforming growth factor-beta 1 in the rat brain: increase after injury and inhibition of astrocyte proliferation. *J Cell Biol* 117:395–400.
- Hunter KE, Sporn MB, Davies AM (1993) Transforming growth factor-betas inhibit mitogen-stimulated proliferation of astrocytes. *Glia* 7:203–211.
- Toru-Delbauffe D, et al. (1990) Effects of transforming growth factor beta 1 on astroglial cells in culture. *J Neurochem* 54:1056–1061.
- Bakin AV, et al. (2005) Smad3-ATF3 signaling mediates TGF-beta suppression of genes encoding Phase II detoxifying proteins. *Free Radical Biol Med* 38:375–387.
- Jankowsky JL, et al. (2004) Mutant presenilins specifically elevate the levels of the 42 residue beta-amyloid peptide in vivo: Evidence for augmentation of a 42-specific gamma secretase. *Hum Mol Genet* 13:159–170.
- Koponen JK, et al. (2007) Umbilical cord blood-derived progenitor cells enhance muscle regeneration in mouse hindlimb ischemia model. *Mol Ther* 15:2172–2177.
- Wild AC, Moinova HR, Mulcahy RT (1999) Regulation of gamma-glutamylcysteine synthetase subunit gene expression by the transcription factor Nrf2. *J Biol Chem* 274:33627–33636.
- Hurttila H, et al. (2008) Oxidative stress-inducible lentiviral vectors for gene therapy. *Gene Ther* 15:1271–1279.
- Ogita K, et al. (2000) Enhanced binding activity of nuclear antioxidant-response element through possible formation of Nrf2/Fos-B complex after in vivo treatment with kainate in murine hippocampus. *Neuropharmacology* 46:580–589.